ARCHIVES OF ELECTRICAL ENGINEERING VOL. 64(3), pp. 441-458 (2015)

DOI 10.2478/aee-2015-0034

Transient recovery voltage analysis for various current breaking mathematical models: shunt reactor and capacitor bank de-energization study

PIOTR ORAMUS, TOMASZ CHMIELEWSKI, TOMASZ KUCZEK, WOJCIECH PIASECKI, MARCIN SZEWCZYK

ABB Corporate Research Center
Starowiślna 13A, 31-038 Kraków, Poland
e-mail: piotr.oramus@pl.abb.com

(Received: 29.09.2014, revised: 11.02.2015)

Abstract: Electric arc is a complex phenomenon occurring during the current interruption process in the power system. Therefore performing digital simulations is often necessary to analyse transient conditions in power system during switching operations. This paper deals with the electric arc modelling and its implementation in simulation software for transient analyses during switching conditions in power system. Cassie, Cassie-Mayr as well as Schwarz-Avdonin equations describing the behaviour of the electric arc during the current interruption process have been implemented in EMTP-ATP simulation software and presented in this paper. The models developed have been used for transient simulations to analyse impact of the particular model and its parameters on Transient Recovery Voltage in different switching scenarios: during shunt reactor switching-off as well as during capacitor bank current switching-off. The selected simulation cases represent typical practical scenarios for inductive and capacitive currents breaking, respectively.

Key words: arc modelling, overvoltages studies, EMTP-ATP program, transients analysis

1. Introduction

Physical phenomena occurring upon current interruption are very complex. For this reason, it is still a challenge to use appropriate arc models for circuit breaker design and insulation coordination studies. The used model should represent non-linear behaviour of the circuit breaker electric arc as well as the interaction between the switching process and the system components. Moreover, since very small time constants are involved, a correct numerical treatment of the arc-circuit problem is an important aspect as well. Various interrupting media with different dielectric strength characteristics are applied in HV circuit breakers depending on particular design, application, price, etc. The dielectric strength determines the maximum electric stress that the dielectric can withstand without breakdown. It is a multi-variable function of the switching process and design of the particular switchgear component.

The general models of the electric arc, such as Mayr/Cassie, are often used in a modified form to reflect the arc voltage condition obtained in the measurement (e.g. the modified Mayr eq. [1]). The switching process can be measured in synthetic circuit, which allows to reproduce the realistic Transient Recovery Voltage (TRV), arc voltage and post-arc current conditions. The approach proposed by Mayr [2] is well suited for vicinity of current zero crossing. Not only the parameters, but the model itself can be modified according to the measured curves of the arc voltage and post-arc current. The example of the modified Mayr and Cassie equations is the Schwarz-Avdonin model [3].

The application of Mayr and Cassie models is recommended by IEC standards for insulation coordination studies to represent the physics of the circuit-breaker [4]. Cassie and Mayr models describe the evolution of the conductance (or resistance) of the electric arc during current interruption process, in accordance with the behaviour of the voltage and current appearing at the circuit breaker terminals. In insulation coordination analyses related to switching overvoltages, the arc equations are implemented in numerical software, such as EMTP-ATP [5]. This article contains the comparison of various electric arc models behaviour in selected simulation cases to investigate the impact of the electric arc model on the transient analysis results for the interruption process of the inductive and capacitive current breaking. The paper is based on this recommendation which is specifically applicable for simulations. Hence, the measurements of switching transients are not object of this analysis. Parameters of the models analysed in this paper are used here based on the research reported in e.g. [1, 3].

2. Inductive and capacitive current switching

The switching capabilities of high-voltage circuit breakers are defined by international standards that also describe the normative laboratory tests (using standard circuits) for inductive and capacitive current breaking [6, 7]. Along with capability of specific current breaking, the overvoltages generated during these operations are studied. The transient system response may be different for various configurations and topologies of the de-energized circuit. These aspects can be analysed through insulation coordination process, with the possible use of various simulation environments. The guidelines regarding modelling aspects as well as definition of the events that should be verified, are well established and described in [4, 8, 9]. In the routine switching study both fault clearing and load rejection scenarios should be considered.

In this paper, switching of capacitive and inductive currents is analysed. These cases were chosen to analysis due to especially difficult conditions of current interruption process (the dielectric withstand of the contact gap can be exceeded just after arc quenching process, what can cause to generate re-ignitions, an in consequence an unsuccessful current breaking operation). According to [8] and [9], switching of capacitive currents involves energization or de-energization of unloaded cables, overhead lines and capacitor banks. For inductive currents, switching operations are typically related to motor starting as well as energization and de-energization of transformers and shunt reactors at no-load state or during inrush current flow.

Large amount of the energy accumulated in the system during the breaking process causes specifically demanding TRV conditions for the breaker due to possible re-ignition and voltage escalation. Moreover, breaking of inductive currents can lead to high frequency overvoltages if the current is chopped. At low currents (a few Amps) the arc becomes unstable, which may result in chopping before its natural zero crossing. This phenomenon may generate high transient overvoltage peak values due to the oscillations of the energy trapped in the oscillatory circuit, which is formed of the equivalent inductance and capacitance of the circuit being switched off [9]. The making procedure of inductive elements is on the other hand more critical from the point of view of the inrush current and possible saturation of other equipment magnetic cores (if are present) [10], however, this is out of scope in this paper as mentioned earlier. For the de-energization process, the typical oscillograms of voltage and current that are present in the system are illustrated in Figure 1. It was assumed here that the arc re-ignition did not occur.

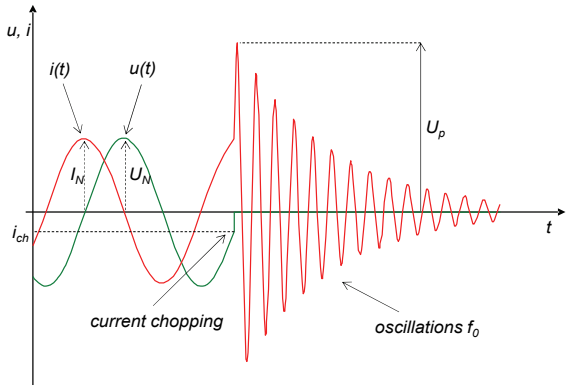

Fig. 1. Breaking of inductive current without arc re-ignitions, $i(t)$ – current, $u(t)$ – voltage, i_{ch} – chopping current, I_N – nominal current peak, U_N – nominal phase voltage, U_p – peak voltage after de-energization, f_0 – frequency of oscillations

Making process of capacitive equipment, such as capacitor banks, can also pose a threat of overvoltages occurrence. Those transients can reach amplitudes as high as 4 p.u. phase-phase which is caused by traveling wave reflections and consecutive arc re-ignitions [9]. However, these aspects are out of the scope of work presented in this paper.

During breaking of capacitive currents the current chopping phenomenon is also present, similarly to the inductive current cases. The main concern upon that process are overvoltages produced due to possible arc re-ignitions [7-9], for example during capacitor bank de-energization. This is due to the fact that during the current breaking process the voltage at the capacitor banks terminals remains constant, and can even further escalate with the consecutive re-strikes, which can exceed the dielectric withstand of the contact gap and in consequence can cause an unsuccessful breaking operation, meaning the dielectric withstand has not been sufficiently restored. The main aspect of this work is the voltage and current waveforms after interruption of capacitor bank current at high voltage level. The typical voltage and current traces without any re-ignitions are presented in Figure 2.

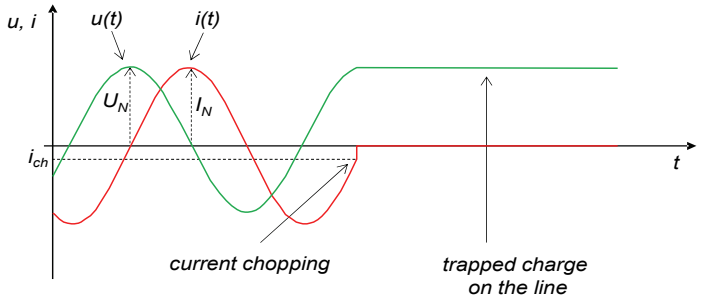

Fig. 2. Breaking of capacitive current without arc re-ignitions, $i(t)$ – current, $u(t)$ – voltage, i_{ch} – chopping current, I_N – nominal current peak, U_N – nominal phase voltage

As shown in Figure 1 and in Figure 2, current is chopped just before natural zero-crossing. It can be noticed that switching operation without any re-ignitions can generate overvoltages, which are overstressing insulation systems of devices installed in HV power system. For this reason, insulation coordination studies are essential to predict dangerous effects of switching transient states occurring in electrical network. For this purpose, development of mathematical electric arc models providing appropriate electric arc representation is necessary. Comparison of various mathematical electric arc models is presented in Section 3.

3. Mathematical electric arc models

In order to analyse switching transient states by means of computer simulations, mathematical models of electric arc have to be implemented into specialized software. Performing overvoltages simulation is possible also using an ideal switch model available in the EMTP-ATP software. However, this approach is only applicable, if the chopping current level can be reasonably estimated. Moreover, application of the ideal switch model does not accurately represent the actual process of current interruption. Thus, in order to improve precision of simulation results, development of more complex models is necessary. In this paper the approach to model arc by means of variable conductance was used as recommended by the IEC Std. [4, 8]. For this purpose, various mathematical models describing electric arc behaviour during switching operation in HV circuit breakers are presented and analysed in this section.

3.1. Ideal switch circuit breaker model

Standard approach on circuit breaker modelling implemented in transient simulation software, e.g. EMTP-ATP, is based on chopping current definition and the so called ideal switch operation. A typical current waveform during interruption process including chopping current phenomenon are illustrated in Figure 1 and in Figure 2. For computation of switching transient states, the value of the chopping current can be estimated for analysed circuit breaker by the following formula [11-14]:

$$i_{ch} = k \cdot \sqrt{N \cdot C}, \tag{1}$$

where: k – chopping number $[\mathrm{A{\cdot}F}]^{-0.5}$, N – number of breaking chambers, C – total capacitance seen from the circuit breaker's terminals [F].

The chopping number k can be described as a characteristic constant of the circuit breaker for various types of quenching medium (except for vacuum circuit breakers). Typical k coefficient values for minimum oil, air blast, and SF_6 circuit breakers are listed in Table 1. Due to fact that chopping number was not explicitly specified, boundary values had to be provided. This was done according to [13]. The influence of the system parameters on the chopping current value is included in equation (1) by means of the equivalent capacitance C [11-14].

Table 1. Circuit breaker chopping numbers [13]

Circuit breaker types	**Chopping number**
[–]	$[\mathrm{A{\cdot}F}]^{-0.5}$
minimum oil	$7 \div 10 \cdot 10^4$
air blast	$15 \div 25 \cdot 10^4$
SF_6	$4 \div 17 \cdot 10^4$

Due to difficulty of accurate chopping current value estimation (dependent on particular circuit breaker design) as well as due to randomness of the electrical arc phenomena, the model basing on that parameter is considered to be a highly simplified approach. More accurate models (such as: Cassie or Mayr models) are able to estimate values of the electric arc conductance during breaking current basing on the characteristic constant parameters of the considered circuit breaker.

3.2. Cassie model

In comparison to the ideal switch presented in Section 3.1, Cassie model, as presented in this section, provides better representation of the electric arc for large values of current. Basically, the Cassie approach includes calculation of electric arc conductance in the time domain basing on parameters characterizing given circuit breaker type. The Cassie formula is presented below as a differential equation describing the arc conductance during the current interruption process [15-17]:

$$\frac{dg_c}{dt} = \frac{1}{\tau_c} \cdot \left(\frac{i_a^2}{u_s^2 \cdot g_c} - g_c \right), \tag{2}$$

where: g_c – arc conductance [S], τ_c – time constant of the arc [s], P_0 – steady-state cooling power of the arc [W], u_s – steady state arc voltage [V], i_a – the arc current [A].

In order to perform analyses using the Cassie model, knowledge of constants given by Equation (2) is necessary. However, their values are strongly dependent on the circuit breaker design. Many parameters of the circuit breaker (contact system design, type of quenching medium, velocity of the contacts movement, etc.) have influence on the values of constant parameters in the Cassie equation. For this reason, estimation of the required parameters has to be performed individually for each type of the circuit breaker analysed. Table 2 shows

exemplary values of the constant parameters for the arc given by the Cassie equation (steady-state cooling power of the arc and steady state arc voltage). The parameters are given for air as well as for SF_6 gas HV circuit breakers.

3.3. Cassie-Mayr model

In order to further improve computations accuracy, together with the previously described Cassie model, the Mayr equation can be implemented to represent phenomena of the electric arc also for small values of current (in the vicinity of the current zero-crossing). The Mayr approach (similarly to Cassie model) allows to calculate the electric arc conductance using constant parameters depending on the circuit breaker design. The Mayr equation is presented below as a differential equation describing arc conductance [2, 16, 17]:

$$\frac{dg_m}{dt} = \frac{1}{\tau_m} \cdot \left(\frac{i_a^2}{P_0} - g_m \right), \tag{3}$$

where: g_m – the arc conductance [S], τ_m – the time constant of the arc [s], P_0 – the steady-state cooling power of the arc [W].

For the high current conditions, the Cassie's portion of the arc voltage is the main part of the total arc voltage. When the current is close to zero, the Mayr's portion describes the arc behaviour more accurately. The arc voltage related to the Mayr part increases just before the current zero crossing and takes over the transient recovery voltage after the current interruption, while the Cassie's portion goes to zero. Hence, the overall process can be represented by the arc conductance given by the two differential models working simultaneously. The total arc resistance is then given by [16, 17]:

$$r_{arc} = \frac{1}{g_{arc}} = \left(\frac{1}{g_c} + \frac{1}{g_m} \right), \tag{4}$$

where: g_c – the arc conductance calculated according to the Cassie equation (2), g_m – the arc conductance calculated according to the Mayr equation (3).

Equation (4) provides good representation of the arc behaviour for low as well as for high current values. The values of constants given in equation (4) are presented in Table 2 for air and SF_6 HV circuit breakers [1].

Table 2. Exemplary values of constants for Cassie and Mayr equations [1]

Circuit breaker type	**Cassie equation**		**Mayr equation**	
	time constant of the arc τ_c	steady state arc voltage u_s	time constant of the arc τ_m	steady-state cooling power of the arc P_0
	[μs]	[kV]	[μs]	[kW]
Air	0.8	2.60	0.124	3.45
SF_6 gas	0.8	2.35	0.22	8.8

3.4. Schwarz-Avdonin model

One of the modified versions of the Cassie-Mayr model is the Schwarz-Avdonin model. This approach is based on the following equation [3, 18, 19]:

$$\frac{dg}{dt} = \frac{1}{\tau(g)} \cdot \left(\frac{i^2}{P(g)} - g \right), \tag{5}$$

where: g – arc conductance [S], i – interrupting current [A], $P(g)$ – arc cooling power dependent on the electric arc conductance [W], $\tau(g)$ – arc thermal time constant dependent on the electric arc conductance [s].

The Schwarz-Avdonin Equation (5), describing arc behaviour has the same general structure as the Cassie-Mayr formula. However, in the Schwarz-Avdonin approach the cooling power P and the thermal time constant τ are conductance-dependent parameters $P(g)$ and $\tau(g)$ respectively. Also, similarly to the Cassie-Mayr approach, the constant parameters given in formula (5) are dependent on other parameters, such as: temperature, circuit breaker design, quenching medium type. The values of the cooling power and thermal time constant can be defined as a function of conductance $f(g)$, according to following dependences:

$$P = P_0 \cdot g^{\beta}, \tag{6}$$

$$\tau = \tau_0 \cdot g^{\alpha}, \tag{7}$$

where: g – arc conductance [S], α – free parameter $[S]^{-1}$, β – free parameter $[S]^{-1}$, P_0 – the arc cooling power constant [W], $\tau(g)$ – the arc thermal time constant [s].

The values of constants used for exemplary HV circuit breaker construction with air and SF_6 quenching medium are listed in Table 3 [3].

Table 3. Values of parameters for HV circuit breakers in Schwarz-Avdonin model [3]

Circuit breaker type	**Arc cooling power P**	**Time constant of the arc τ_m**	**α coefficient**	**β coefficient**
	[MW]	[μs]	[–]	[–]
SF_6 gas	4	1.5	0.17	0.68
Air	16	6	0.20	0.50

Depending on the difference between the input (power) and the cooling thermal power, the arc temperature and conductivity is either going to increase or decrease.

4. Modelling and case studies

4.1. Modelling

The study presented in this paper covers two scenarios namely breaking of shunt reactor rated current and de-energization of unloaded overhead line. For that purpose two models of arbitrary chosen 400 kV network were developed in EMTP-ATP simulations software.

In order to obtain reliable simulation results it is essential that the elements of the system are properly represented by their equivalent models. Therefore, the modelling approach described in detail in this section was mostly based on the guidelines given by IEC Standard [4]. The diagram of the simulated network is depicted in Figure 3.

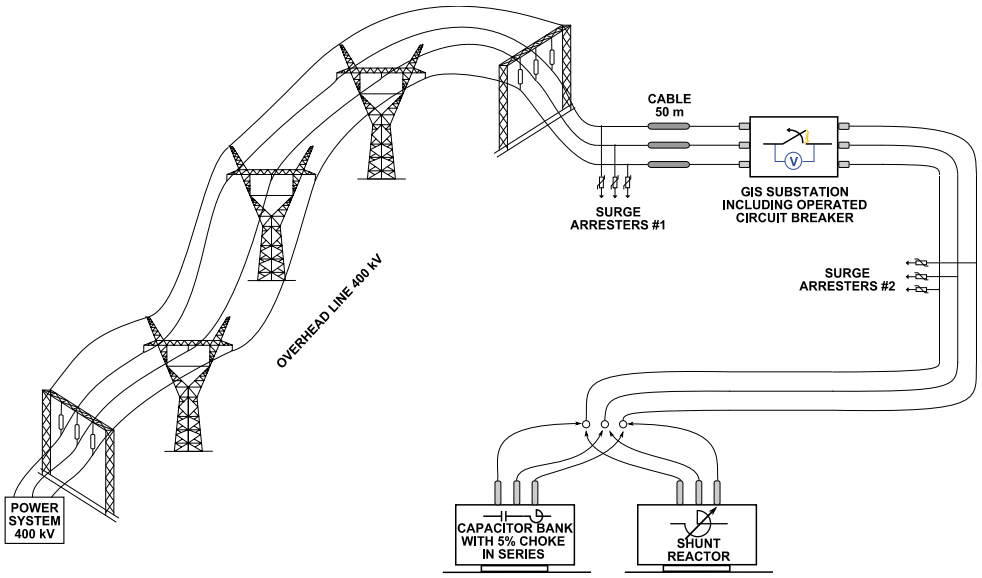

Fig. 3. General diagram of the modelled system

Since the analyses presented in this paper address primarily slow front overvoltages, therefore the model was built based on components presented below.

AC network was modelled as an equivalent element comprising an ideal 50 Hz sinusoidal source complemented with the series RL element that reflects the short-circuit parameters of the utility grid (S_k'' = 40000 MVA, X/R = 10) [11].

The overhead line and cable models for these type of studies are required to be frequency dependent distributed parameters elements. For this purpose, JMarti line type model was applied [20]. It accurately represents the behaviour of the line in wide range of frequencies, taking into account such phenomena as skin effect and wave reflections. The overhead line is considered to be ideally transposed whereas the three single-core cables are arranged in a flat formation, placed 1 meter underground, with the spacing equal to double the diameter of the cable. Both models were developed based on the geometrical parameters as well as the electrical data. The detailed data of the overhead line employed in this study are presented in Figure 4 [21].

Parameters of HV cable used for insulation coordination studies were taken from the manufacturer catalogue [22], as listed in Table 4.

The components of the Gas-Insulated Switchgear substation (GIS) substation were represented using surge impedances modelling GIS busducts and lumped capacitances as recommended by [4]. The values of the capacitances are presented in Table 5 [23].

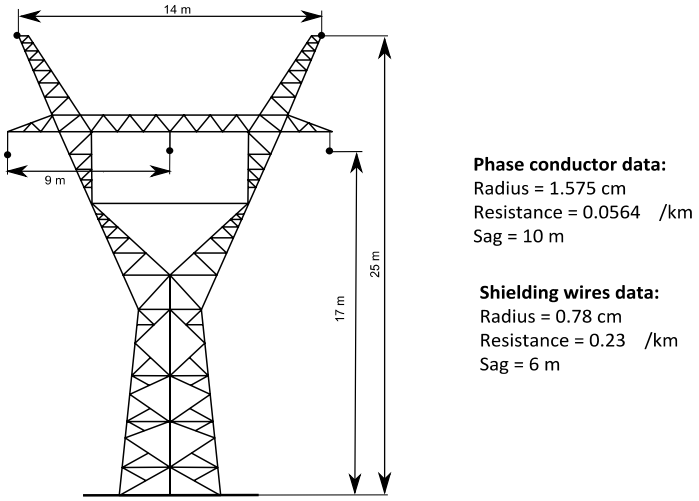

Fig. 4. The layout of overhead line tower used in simulations

Table 4. HV cable parameters [22]

Conductor diameter	Insulation thickness	Diameter over insulation	Outer diameter of cable	Conductor cross-section	Screen cross-section	Insulation relative permittivity	Core and screen material resistivity
[mm]				[mm^2]		[–]	[Ω · m]
54.4	27.0	113.4	132.8	2000	185	2.4	$1.7 \cdot 10^{-8}$

Table 5. Values of capacitances used to simulations

Type of equipment	Value	Unit
busbar	50	[pF/m]
circuit breaker	2×50	[pF]
voltage transformer	80	

The shunt reactor is assumed to deliver 60 MVA at $U_{L-L} = 400$ kV. Its nonlinear magnetization characteristic was implemented assuming 1.5 p.u. knee voltage and 30% slope beyond this value (in the deep saturation region) [4]. The damping resistance of 2.6 Ω was applied in series in order to represent the shunt reactor losses.

Surge arresters were modelled as nonlinear elements based on their 30/60 μs voltage-current (V-I) characteristics presented in Table 6.

The circuit breaker was modelled using the time variable resistor controlled with the EMTP-ATP scripting language MODELS. For this purpose, the Mayr, the Cassie-Mayr, and the Schwarz-Avdonin equations were implemented, describing the behaviour of the electric arc during the current interruption process in different system conditions. This approach allows one to control the variable resistance *R(TACS)* according to the assumptions given by the particular models.

Table 6. V-I characteristics of analysed surge arresters

Current	**Surge Arrester #1**	**Surge Arrester #2**
	residual voltage	
[kA]	[kV]	
0.5	–	743
1	692	764
2	712	788
3	725	–

Although Mayr and Cassie models were first introduced for the electric arc at relatively low voltage system conditions, they have eventually found broad application in modeling of medium- and high-voltage switchgear. The approach on modeling of the electric arc using Mayr and Cassie models for HV circuit breakers is presented e.g. in: [1, 3, 18], together with the models parameters for HV systems. The Mayr-Cassie model is recommended in IEC Standard [4] for insulation coordination studies in HV systems. Detailed description of the models considered are presented in Section 3. Separate approach was used for the model of the ideal switch with predefined chopping current level, which is available in the default program library. The chopping current values were calculated according to Equation (1), which provided chopping current levels for minimum and maximum values of the chopping number. Detailed description of the ideal time controlled switch *TSWITCH* is given in [5].

4.2. Case studies

In order to compare simulation results obtained from calculations with the use of various models of electric arc during switching transient conditions, different cases were analysed. The list containing all of the considered simulation cases performed in ETMP-ATP is presented in Table 7.

Table 7. Considered cases for simulations

Case	**Type of breaker model**	**Type of operation**	**Operation time instant**
1i* and 1c**	Cassie	breaking of shunt reactor rated current (inductive) or breaking of unloaded line current (capacitive)	$t = 0.04$ s
2i and 2c	Schwartz-Avdonin		
3i and 3c	Cassie-Mayr		
4i and 4c	Ideal switch $i_{ch} = x$		
5i and 5c	Ideal switch $i_{ch} = y$		

*i – case showing inductive current breaking – shunt reactor, *c – case showing capacitive current breaking – capacitor bank

As the goal of this work was to analyse transient overvoltage response during de-energization of capacitive and inductive currents in high voltage networks, the following representative de-energization scenarios were selected:

- For capacitive current – de-energization of high voltage capacitor bank,
- For inductive current – de-energization of high voltage shunt reactor.

Analysis of inductive current breaking was performed for the network presented in Figure 3. The capacitive current breaking was analysed for the circuit in which the shunt reactor is replaced with the grounded wye connected capacitor bank (C_Y = 1 μF). The capacitors are connected in series with 5% damping choke.

5. Simulation results

Simulated results of the voltage and current extracted from the cases described in Table 6 are presented in this section. Figures illustrating TRV between the circuit breaker contacts and the current in the system are presented in Appendix A (Figs. 1-10). Due to the fact that the current breaking process is a main focus of this paper, the near zero region of the current upon the contacts separation is accordingly magnified. The simulation results (including the peak value of the voltage just after current interruption) are summarized in Table 8 (TRV was presented both in kV values, as well as in p. u. – it was calculated in reference of based component of network voltage).

Table 8. Simulation results (first peak just after current interruption)

Case	Interrupted device	Type of breaker model	TRV (kV_{peak})	TRV (p.u.)
1i	shunt reactor	Cassie	613	1.88
2i		Schwartz-Avdonin	622	1.91
3i		Cassie-Mayr	673	2.06
4i		Ideal switch i_{ch} = 1.34 A	628	1.93
5i		Ideal switch i_{ch} = 5.71 A	805	2.47
1c	capacitor bank	Cassie	38	0.12
2c		Schwartz-Avdonin	44	0.13
3c		Cassie-Mayr	69	0.21
4c		Ideal switch i_{ch} = 1.34 A	51	0.16
5c		Ideal switch i_{ch} = 5.71 A	132	0.40

As shown in Table 8, the values of TRV first peaks just after current interruption are significantly greater for inductive current interruption in comparison to the breaking capacitive current cases. The discussion of the results is attached in section 6 – Conclusions.

6. Conclusions

The conclusions drawn from the analyses performed in this paper are summarized below:

- EMTP-ATP simulation software allows for effective and efficient implementation of arc models given by means of differential equations,

- the study presented herein has shown that all four investigated models of circuit breakers are able to successfully interrupt the inductive and capacitive currents in the analysed switching conditions,
- it is also clear that the result of the breaking process in terms of TRV magnitude and voltage shape differ for all models, however, the results of TRV calculated for cases 1i – 4i and 1c – 4c exhibit similar peak values,
- comparison of the ideal switch operation for both capacitive and inductive current interruption is very straightforward: the higher the chopping current, the higher the generated overvoltages,
- the frequency of oscillations that occur after contacts separations are dependent mostly on the circuit that is being interrupted and not on the type of the circuit breaker model employed,
- all types of circuit breaker models presented herein are applicable for insulation coordination study, the final choice should be made based on the trade-off between the quality of the possessed input data and the desired complexity of analysis,
- complexity of input parameters implementation are different for each model, which can suggest diversity of simulation results for various models. Nonetheless the recorded TRV during simulation of arc based models (Cassie, Cassie-Mayr and Schwartz-Avdonin) were fairly similar; the maximum results difference was as high as 60 kV_{peak} for inductive current interruption and 31 kV_{peak} for capacitive current breaking; simulation results also indicate that application of ideal switch with accordingly estimated value of the chopping current can be alternative simplification during insulation coordination studies,
- from insulation coordination viewpoint, calculations performed using Cassie-Mayr model in switching analyses seem to be the most appropriate; this model is recommended by IEC IEC 60071-4:2004standard, and provides good arc behaviour representation in transient states analyses),
- values of calculated TRV are larger for shunt reactor study in comparison to capacitor bank study, which shows that inductive current interruption is more critical case for devices installed in electric power network (from insulation coordination viewpoint),
- one has to bear in mind that all of the circuit breaker models require specific parameters that can be obtained from the measurement of arc voltage and post-arc currents in real test settings.

Appendix A

In this section, simulation results of the current breaking process are shown, performed with the use of various arc models as presented in section 3. The following waveforms were calculated for inductive current breaking: current of the shunt reactor, magnified current of the shunt reactor and TRV between circuit breaker contacts. For simulation results of capacitive current, also zoomed oscillations of TRV are presented. For all of the waveforms presented in this section the same phase sequence is used, which is according to the description given in Figure 1.

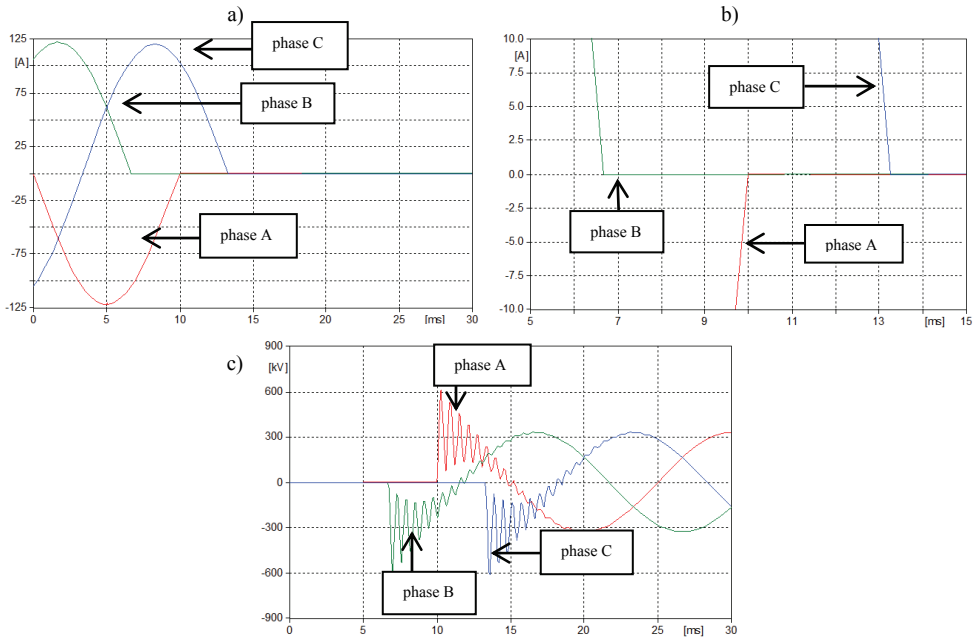

Fig. 1. The simulation results of inductive current breaking using Cassie arc model: a) current of the shunt reactor, b) magnified current of the shunt reactor, c) TRV between circuit breaker contacts

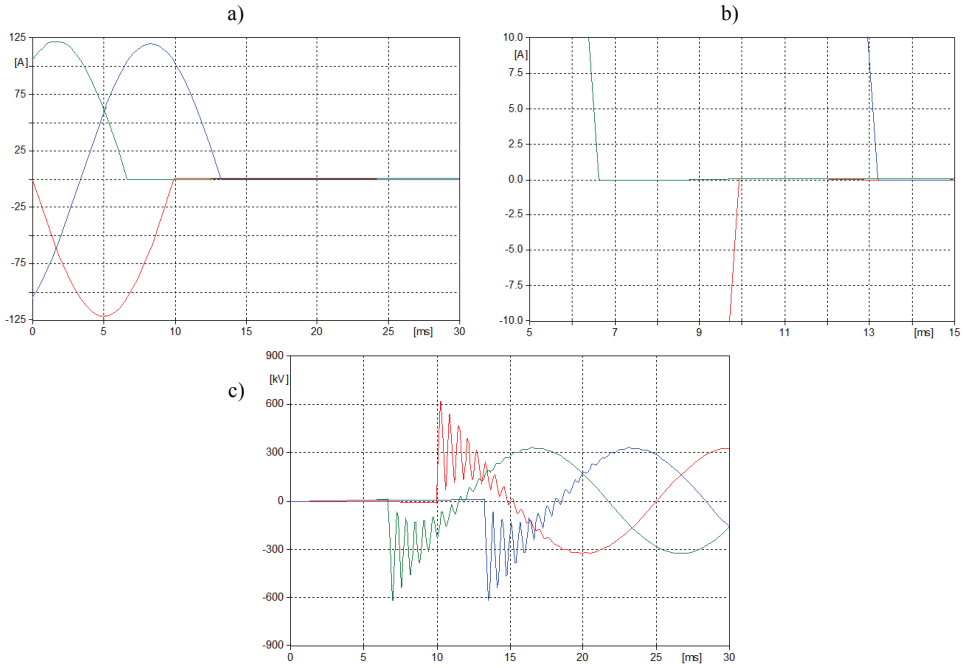

Fig. 2. The simulation results of inductive current breaking using Schwartz-Avdonin arc model: a) current of the shunt reactor, b) magnified current of the shunt reactor, c) TRV between circuit breaker contacts

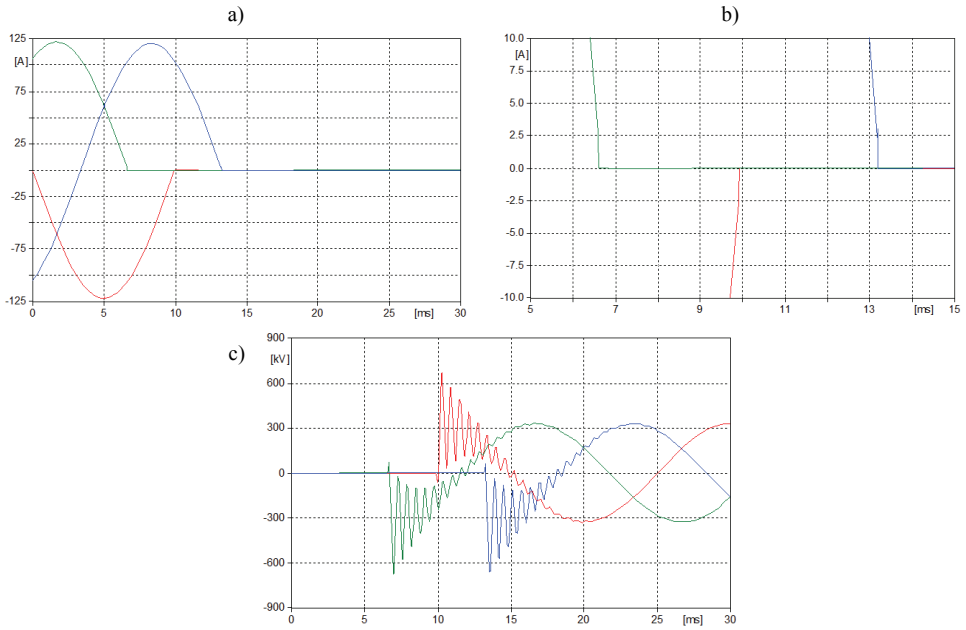

Fig. 3. The simulation results of inductive current breaking using Cassie-Mayr arc model: a) current of the shunt reactor, b) magnified current of the shunt reactor, c) TRV between circuit breaker contacts

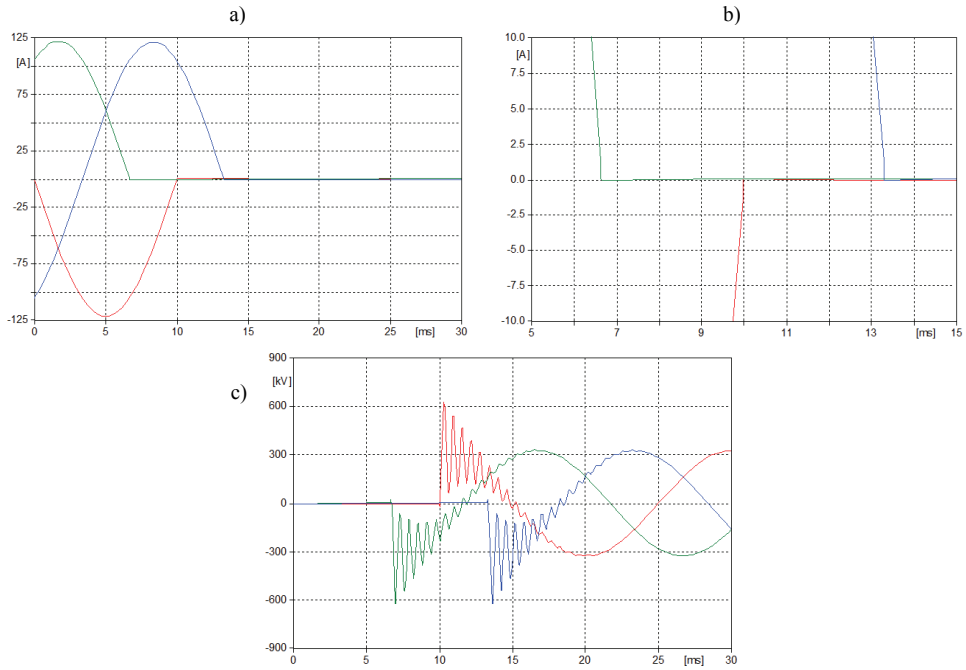

Fig. 4. The simulation results of inductive current breaking using ideal switch i_{ch} = 1.34 A: a) current of the shunt reactor, b) magnified current of the shunt reactor, c) TRV between circuit breaker contacts

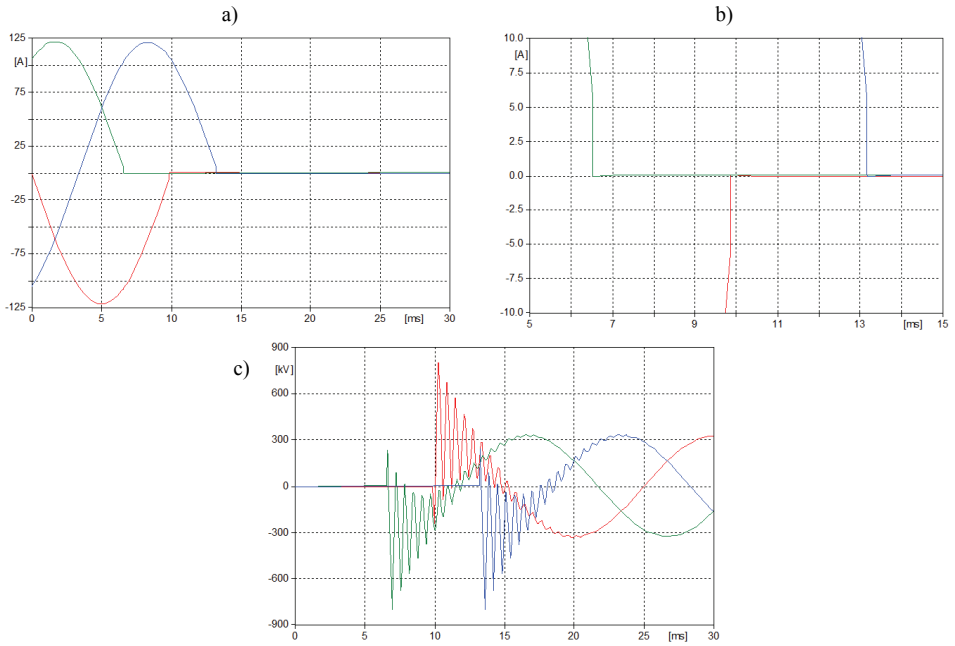

Fig. 5. The simulation results of inductive current breaking using ideal switch i_{ch} = 5.71 A: a) current of the shunt reactor, b) magnified current of the shunt reactor, c) TRV between circuit breaker contacts

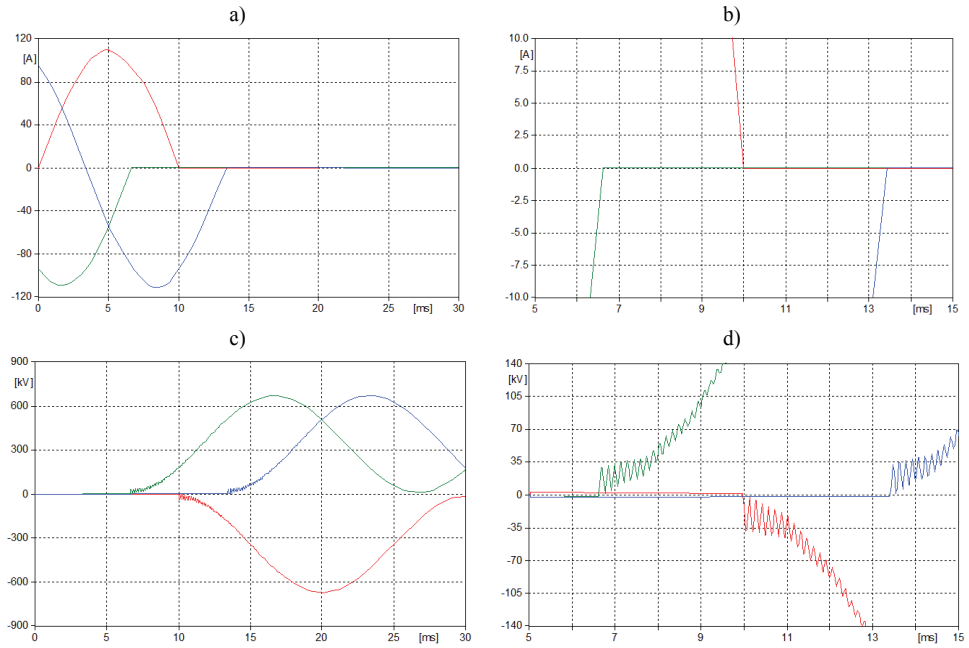

Fig. 6. The simulation results of capacitive current breaking using Cassie arc model: a) current of the shunt reactor, b) magnified current of the shunt reactor, c) TRV between circuit breaker contacts, d) zoomed oscillations of TRV presented in figure c

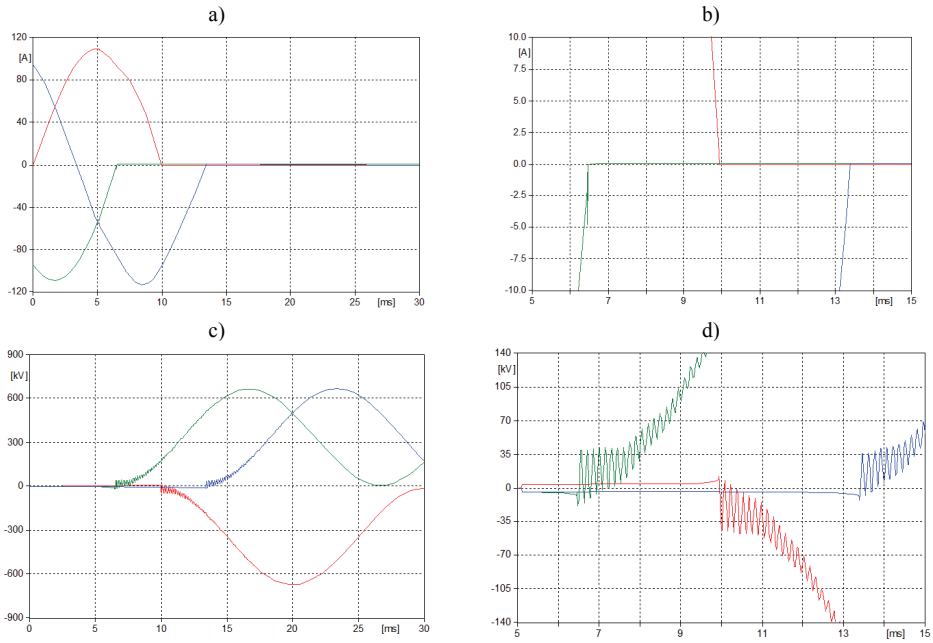

Fig. 7. The simulation results of capacitive current breaking using Schwartz-Avdonin arc model: a) current of the shunt reactor, b) magnified current of the shunt reactor, c) TRV between circuit breaker contacts, d) zoomed oscillations of TRV presented in figure c

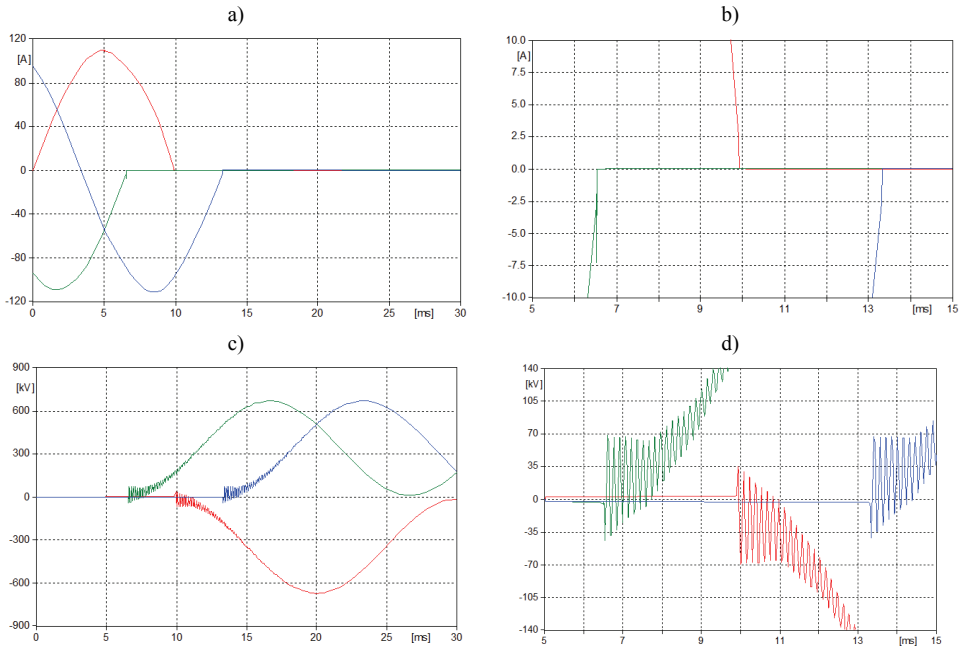

Fig. 8. The simulation results of capacitive current breaking using Cassie-Mayr arc model: a) current of the shunt reactor, b) magnified current of the shunt reactor, c) TRV between circuit breaker contacts, d) zoomed oscillations of TRV presented in figure c

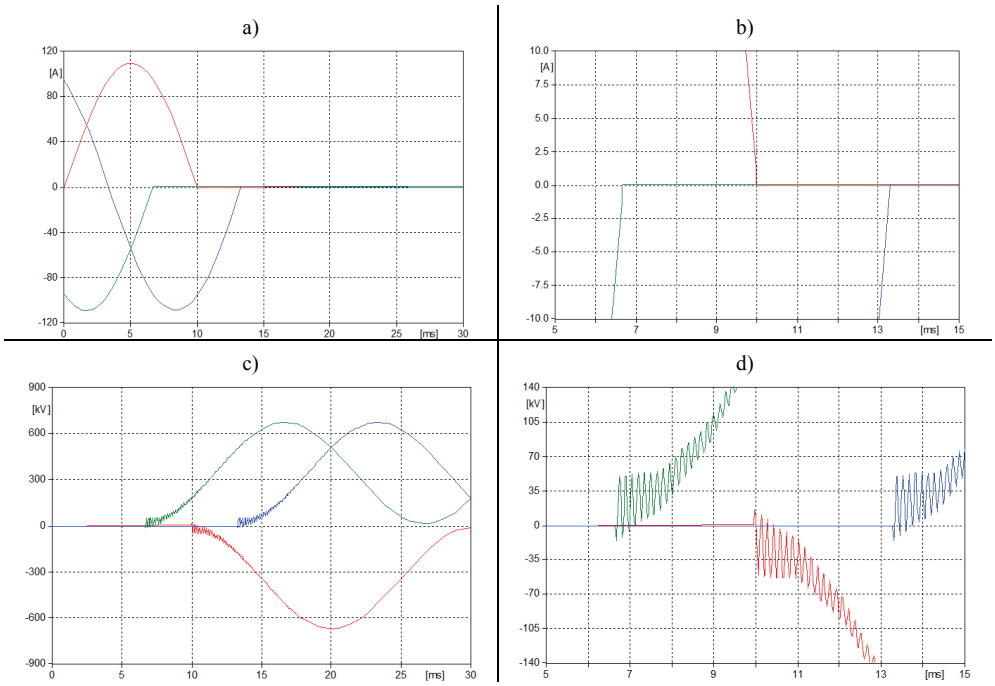

Fig. 9. The simulation results of capacitive current breaking using ideal switch i_{ch} = 1.34 A: a) current of the shunt reactor, b) magnified current of the shunt reactor, c) TRV between circuit breaker contacts, d) zoomed oscillations of TRV presented in figure c

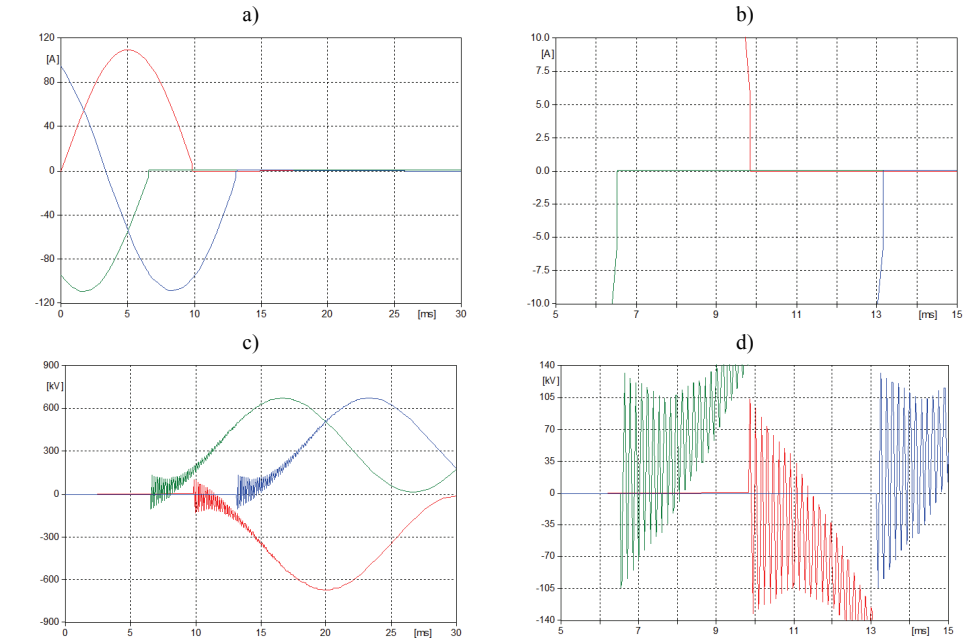

Fig. 10. The simulation results of capacitive current breaking using ideal switch i_{ch} = 5.71 A: a) current of the shunt reactor, b) magnified current of the shunt reactor, c) TRV between circuit breaker contacts, d) zoomed oscillations of TRV presented in figure c

References

[1] Habedank U., *Application of a New Arc Model for the Evaluation of Short-Circuit Breaking Tests*. IEEE Transactions on Power Delivery 8(4), (1993).

[2] Mayr O., *Beitrag zur theorie der statischen und der dynamischen lichtbogens*. Archiv fuer Elektrotechnik, Berlin, Germany 37: 588-608 (1943).

[3] Hutter S., Uglešić I., *Universal arc resistance model "ZAGREB" for EMTP*.

[4] IEC 60071-4:2004: *Insulation coordination – Part 4: Computational guide to insulation co-ordination and modelling of electrical networks.*

[5] Meyer W.S., Liu T.-H, *Alternative Transients Program (ATP) Rule Book.* Canadian/American EMTP User Group, 1987-2000 (distributed by EEUG).

[6] IEC 62271-110: *High-voltage switchgear and controlgear – Part 110: Inductive load switching.*

[7] IEC 62271-110: *High-voltage switchgear and controlgear – Part 100: Alternating-current circuit-breakers.*

[8] IEC 60071-2: *2004. Insulation coordination – Part 2: 2.*

[9] IEEE Std 1313.2-1999, *IEEE Guide for the Application of Insulation Coordination.*

[10] IEC-60076-8: *Power transformers – Part 8 Application guide.*

[11] IEC-60076-5: *Power transformers – Part 5 Ability to withstand short circuit.*

[12] Portela C.M., Morais S.A., Teixeira J.S., *Circuit-breaker behaviour in reactor switching: applicability and limitations of the concept of chopping number.* Power Delivery, IEEE Transactions on 3(3): 1009-1021 (1988).

[13] ABB Technical guide: http://www05.abb.com/global/scot/scot245.nsf/veritydisplay/26886facea44b7b1c1257cec0046a07c/$file/1HSM%209543%2023-02en%20Live%20Tank%20Circuit%20Breaker%20-%20Application%20Guide%20Ed1.2.pdf, accessed October 2014

[14] Chang G.W., Huang H.M., Lai J.H., *Modeling SF6 Circuit Breaker for Characterizing Shunt Reactor Switching Transients*. IEEE Trans. on Power Delivery 22(3): 1533-1540 (2007).

[15] Cassie A.M., *Arc rupture and circit severity: a new theory*. Proceeding of Conference Internationale des Grands Reseaux Electriques a Haute Tension, Paris, France, pp. 1-14 (1932).

[16] Ala G., Inzerillo M., *An improved circuit-breaker model in MODELS language for ATP-EMTP code.* IPST Proceedings (1999).

[17] Bizjak G., Zunko P., Povh D., *Circuit Breaker Model for Digital Simulation Based on Mayr's and Cassie's Differential Arc Equations* (1995).

[18] P.H. Schavemakerand L. van der Sluis, *The Arc Model Blockset.* Proceedings of the Second IASTED International Conference, June 25-28, Greece (2002).

[19] Filipović-Grčić B., Uglešić I., Filipović-Grčić D, *Analysis of Transient Recovery Voltage in 400 kV SF6 Circuit Breaker Due to Transmission Line Faults*. International Review of Electrical Engineering; Sep/Oct 2011 Part B 6(5): 2652.

[20] Marti J.R., *Accurate Modelling of Frequency-Dependent Transmission Lines in Electromagnetic Transient Simulations*. IEEE Transactions on Power Apparatus and Systems PAS-101(1): 147-157 (1982).

[21] CIGRE WG 33.0: *Guide to procedure for estimating the lightning performance of transmission line.* (1991).

[22] ABB technical data sheet: http://www02.abb.com/global/gad/gad02181.nsf/0/a8a42f36692365dcc1257 a62003101ce/$file/XLPE+Land+Cable+Systems+-+User%C2%B4s+Guide.pdf, accessed October (2014).

[23] IEEE Std C37.011™-2005: *Application Guide for Transient Recovery Voltage for AC High-Voltage Circuit Breakers.*